Cluster fullerenes and fullerene clusters

Helmut Hermann, Matthias Krause, Petra Georgi, Jens Noack, Andrei Touzik, Pavel Janda, Steffen Oswald, Norbert Mattern, Lothar Dunsch

In the second decennium of fullerene research the role of clusters in fullerene formation as well as in nano-structuring processes is increasingly recognised. It is demonstrated here that molecular clusters inside carbon cages selectively stabilize endohedral fullerenes. As a consequence nitride cluster fullerenes were obtained as main fullerene product in arc synthesis. On the other hand electrochemical reduction of ordered C_{60} layers produces large fullerene clusters. Here the formation of nanometre scale structures in alkali doped fullerene layers is simulated by Monte Carlo calculations. It is shown that the decomposition mechanism is controlled by electrostatic interactions of fullerene and potassium ions and electronic shell interactions of the fullerenes. Quantum molecular dynamics simulations explain electrochemical processes at the interface between the fullerene layer and the electrolyte.

I. Nitride clusters in fullerene cages

Due to their unique electronic and geometric properties fullerenes are in the focus of fundamental and applied materials research since the first preparation of macroscopic C_{60} quantities by Krätschmer et al. in 1990 [1]. The ability to encage atoms and small molecules opened the door to new structures which are highly reactive under standard conditions. Up to now low production yields and a time consuming multi stage separation hampered the search for applications of endohedral fullerenes.

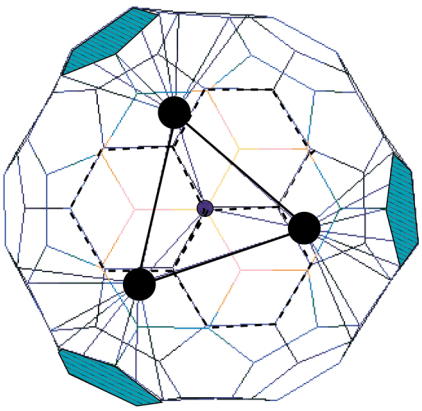

Fig. 1: Calculated molecular structure of $Sc_3N@C_{80}$, reproduced from [4]; large black circles - scandium atoms, small blue circle - nitrogen; C_{80} pentagons closest to the Sc atoms are blue colored; Sc-C and C-C bonds are marked as solid lines

Fullerenes with a triscandium nitride cluster inside as for instance $Sc_3N@C_{80}$ (Fig. 1) have been discovered in 1999, when molecular nitrogen was entering a fullerene reactor accidentally [2]. In our present work the influence of the reactor atmosphere on the fullerene formation and distribution has been studied systematically. Various nitrogen sources in combination with different group 3 and rare earth metals have been investigated. A significant enhancement of the $Sc_3N@C_{80}$ yield in the fullerene extract was first obtained replacing N_2 by calcium carbamide. Even a selective $Sc_3N@C_{80}$ formation with relative yields up to 90 % was achieved by the use of ammonia gas. Our „reactive atmosphere fullerene burning method“ has been successfully applied to produce other trimetal nitride fullerenes, e.g. $Ho_3N@C_{80}$, $Er_3N@C_{80}$ or $Er_2Sc@C_{80}$ as the main fullerene structure in the soot extract [3]. This is illustrated by the high-performance liquid chromatogram in Fig. 2, which is strongly dominated by the $Ho_3N@C_{80}$ peak. By a single extraction step to remove hydrocarbon byproducts these endohedrals are available in reasonable purities. To provide analytical grade fullerenes only one chromatographic separation step is required, compared to the multistage standard technique for the isolation of endohedral fullerenes. Our approach represents an important progress towards a low cost synthesis of these fascinating structures.

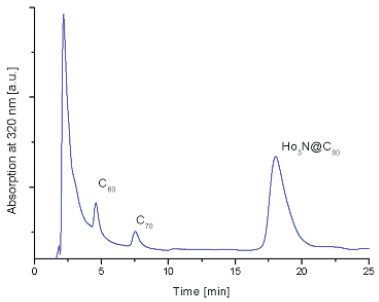

Fig. 2: High performance liquid chromatogram of a fullerene soot extract from an arc synthesis with Ho metal and a reactive NH_3 atmosphere; 4.6 x 25 mm buckyprep column, 1.6 mL/ min flow rate, 200 µL injection volume, toluene eluent; the exponential background is due to hydrocarbon impurities

The improved synthesis is the precondition for further investigations of the geometric and electronic structure of new endohedral fullerenes in dependence on the metal and cage size. So far $Sc_3N@C_{80}$, $Y_3N@C_{80}$, and $Ho_3N@C_{80}$ were studied in detail. A comparison of

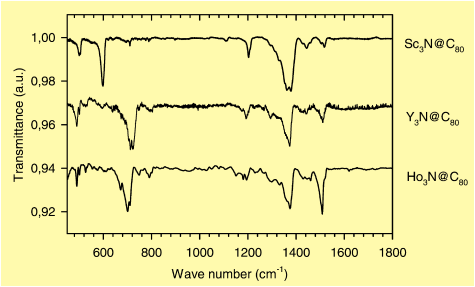

their FTIR spectra is shown in Fig. 3. Although a carbon cage with 80 atoms has 234 vibrational degrees of freedom, only a small number of lines is infrared active for the three structures. In their majority these lines show a clusterlike pattern around a few centres of gravity. It is to

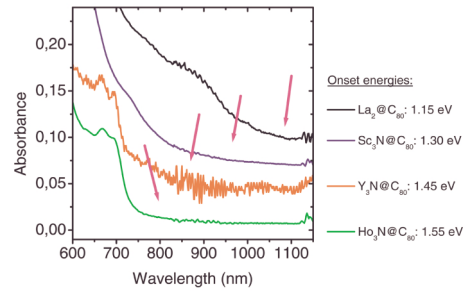

be concluded that $Sc_3N@C_{80}$, $Y_3N@C_{80}$, and $Ho_3N@C_{80}$ prefer the C_{80} cage isomer with icosahedral symmetry, which is slightly distorted by the encaged cluster. In Fig. 4 the onset range of the optical absorption spectra for three $M_3N@C_{80}$ fullerenes is compared to the response of the „classical“ dimetallofullerene $La_2@C_{80}$. All four structures have onset energies above 1 eV and belong to the group of large bandgap fullerenes. The additional significant stabilisation in the order of 0.15 to 0.40 eV is due to the encapsulation of trimetal nitride clusters. Thus it is an intrinsic property of encaged molecular clusters to stabilize fullerene structures as a whole.

II. Structure formation with fullerene molecules: Nanometre scale electrodes on fulleride layers

Alkali metal fullerides form a series of crystalline phases based on simple cubic and face-centred symmetries [5]. The electronic structure and electric properties depend strongly on the crystal structure and the composition A_xC_{60}, A = Na, K, Rb, Cs, $0 \le x \le 6$. Both metallic and insulating behaviour including a metal-insulator phase transition in KC_{60} [6] have been observed. The discovery of superconductivity [7] in doped C_{60} has activated extensive scientific work on this type of material.

One of the most interesting aspects of alkali metal fullerides is the formation of nanometre-scale structures [8]. Recently, Janda showed that nano-electrodes can be prepared by electrochemical copper deposition on nanostructured potassium doped fulleride layers [9]. These experiments have raised questions concerning phase stability, cluster formation, decomposition, and local properties of the layers. Here we summarize experimental results on nanostructure formation on potassium fulleride layers during electrochemical doping and give a theoretical explanation based on molecular dynamics (MD) and Monte-Carlo (MC) simulations.

Potassium doped nanostructured fullerene layers are characterized by a cluster size of about 20 nm [8]. The mean potassium content of the layers is between 0.1 and 0.5 at% [10]. As a consequence of the electrochemical treatment the samples contain also hydrogen and oxygen (Fig.5). As compared to the initial fcc C_{60} layer, the C_{60}-C_{60} distances in

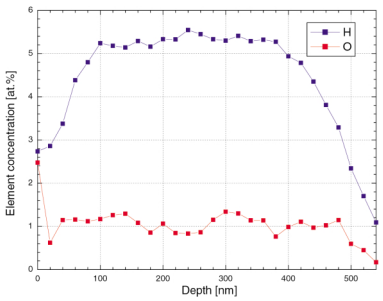

the doped samples are larger and their correlation length is considerably reduced. This is shown by the shift and the broadening of the X-ray diffraction line at about 10.5° in Fig.6. The result of electrochemical copper deposition on a doped C_{60} layer consists in an array of

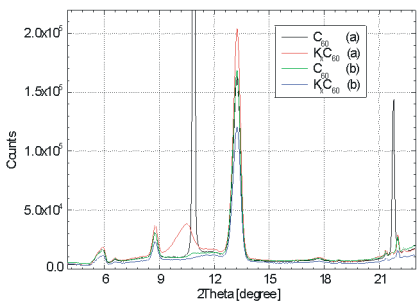

Fig. 3: FTIR spectra of $Sc_3N@C_{80}$, $Y_3N@C_{80}$, and $Ho_3N@C_{80}$ films on KBr single crystal substrates; 293 K, 3 mbar, 2 cm^{-1} resolution, 2000 accumulations; the strong absorption of the $Ho_3N@C_{80}$ sample at 1507 cm^{-1} is due to remaining CS_2 solvent

Fig. 4: Vis/NIR absorption spectra of $La_2@C_{80}$, $Sc_3N@C_{80}$, $Y_3N@C_{80}$, and $Ho_3N@C_{80}$ in the onset region, ca. 10^{-4} mol/L solutions in toluene, 10 mm layer thickness, 2 nm resolution; the arrows mark the onsets

Fig. 5: Depth profiles of hydrogen and oxygen concentration of a doped C_{60} layer measured by heavy ion elastic recoil detection analysis

Fig. 6: X-ray diffraction diagrams of undoped (black curve, a) and doped (red curve, a) C_{60} layers deposited on highly oriented pyrolytic graphite substrates. Curves b were taken from the backside of the substrate and characterize the pure graphite

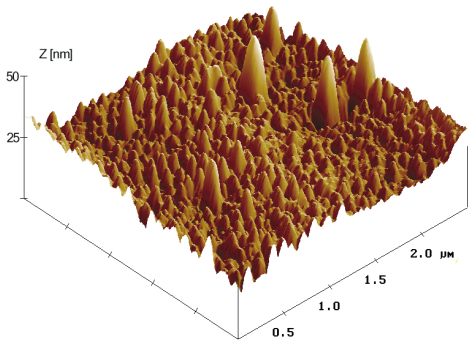

Fig. 7: Copper clusters deposited electrochemically on nanostructured potassium fulleride layers

nanometre scale electrodes (Fig.7). The lateral size of the copper clusters corresponds to the characteristic dimension of the nanostructures developed in the fulleride layers during the doping process. With respect to the height, two types of clusters are identified.

Our MD simulations are based on a density-functional tight-binding method [11]. Fig.8 shows a snapshot of the simulated fullerene-electrolyte interface as it is realized during the doping process. Potassium ions penetrate in the fullerene layer occupying both octahedral and tetrahedral holes of the fcc fullerene lattice. Water molecules decompose and are incorporated in the fullerene layer. The latter result corresponds qualitatively to the H and O content determined experimentally (Fig.5). The MD method is, due to the sophisticated quantum mechanical approach, suitable to take into account only few hundreds of atoms. For the simulation of the formation of the observed nanostructures about 10^6 particles (fullerenes and potassium ions) must be taken into account. This is done by kinetic MC calculations. We estimated the relevant interactions and found that electrostatic (Madelung) contributions of the ions and the electronic-shell repulsion of the fullerenes have to be included in the MC simulations [12]. Starting from both homogeneous and gradient-like random distributions of potassium ions on the octahedral and tetrahedral holes of fcc fullerene lattices the evolution of the systems was simulated over about 10^7 MC steps. The systems decompose into potassium-free and potassium-rich regions. The evolution of the mean size of the potassium-rich (K_3C_{60}) particles is shown in Fig.9. The final size depends on the mean potassium concentration and agrees quantitatively with the experimental data. Since the K_3C_{60} phase is metallic it is of special interest for the understanding of the electrochemical metallization experiments. The copper clusters are deposited on those sites of

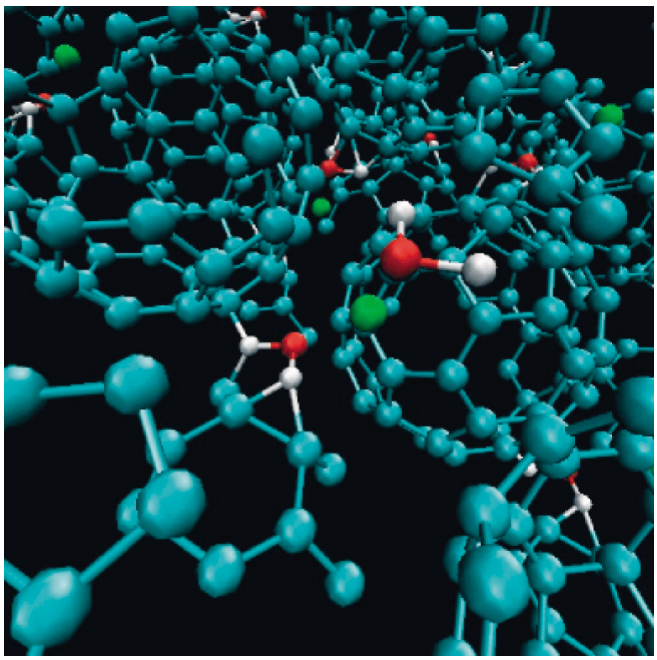

Fig. 8: Snapshot of the arrangement of fullerenes, molecules and ions at the interface between fullerene layer and electrolyte. Green - carbon atoms, yellow - potassium, red - oxygen, white - hydrogen

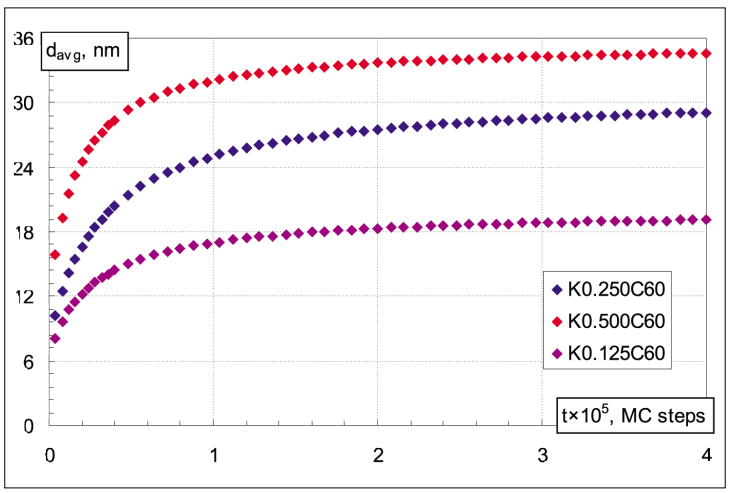

FFig. 9: Evolution of the mean diameter of K_3C_{60} particles versus number of Monte Carlo steps for different mean potassium concentrations

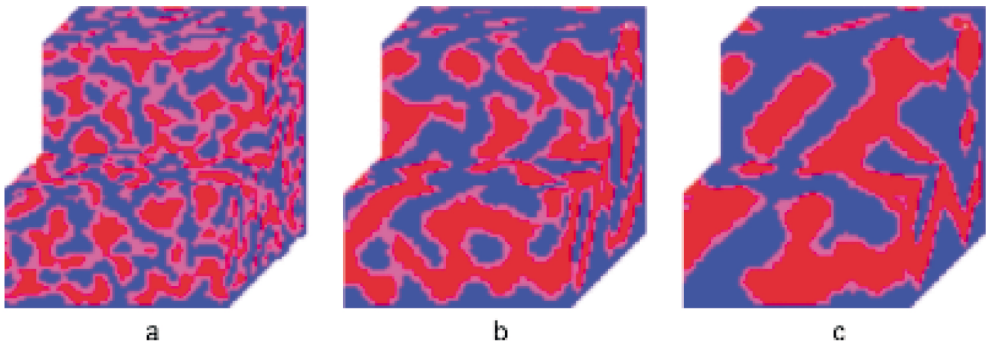

Fig. 10: Decomposition of $K_{0.5}C_{60}$ layer into pure C_{60} regions (blue) and metallic K_3C_{60} particles (red) after 10^3 (a), 10^4 (b) and 10^5 (c) Monte Carlo steps. Metallic percolation paths appear connecting bottom and top of the layer

the layer surface where metallic regions appear. The big clusters (see Fig.9) grow on metallic K_3C_{60} regions which are connected to the electrode on the bottom of the nanostructured fulleride layer by metallic percolations paths illustrated in Fig.10.

The theoretical results obtained from both quantum mechanical atomistic methods and large scale kinetic Monte Carlo simulations give an explanation for the experimentally observed nanostructures on fulleride layers and offer the opportunity to control mean size and distribution of nanometre scale electrodes.

References

[1] W. Krätschmer, L.D. Lamb, K. Fostiropoulus, D.R. Huffman, Nature 347 (1990) 354
[2] S. Stevenson, G. Rice, T. Glass, K. Harich, F. Cromer, M.R. Jordan, J. Craft, E. Hajdu, R. Bible, M.M. Olmstead, K. Maitra, A.J. Fisher, A.L. Balch, H.C. Dorn, Nature 401 (1999) 55
[3] L. Dunsch, P. Georgi, F. Ziegs, H. Zöller, patent claim 2002
[4] M. Krause, H. Kuzmany, P. Georgi, L. Dunsch, K. Vietze, G. Seifert, J. Chem. Phys. 115 (2001) 6596
[5] D. M. Poirier, D. W. Owens, J. H. Weaver, Phys. Rev. B 51 (1995) 1830
[6] C. Coulon et al., Phys. Rev. Lett. 86 (2001) 4346
[7] D. Hebard et al., Nature 350 (1991) 600
[8] P. Janda, T. Krieg, L. Dunsch, Adv. Mater. 10 (1998) 1434
[9] A. Touzik, H. Hermann, P. Janda, L. Dunsch, K. Wetzig, Europhys. Lett. 60 (2002) 411
[10] S. Oswald, P. Janda, L. Dunsch, Mikrochim. Acta 141 (2003) 1
[11] D. Porezag, T. Frauenheim, T. Köhler, G. Seifert, R. Kaschner, Phys. Rev. B 51 (1995) 12947
[12] A. Touzik, H. Hermann, K. Wetzig, Phys. Rev. B 66 (2002) 75403

Cooperation

J. Heyrovský Institute Prague
TU Dresden
Universität Wien
FZ Rossendorf

Funded by

DFG
EU TMR project „Fullprop“